Electrical Power and Energy Systems 68 (2015) 345–355

Contents lists available at ScienceDirect

Electrical Power and Energy Systems

journal homepage: www.elsevier.com/locate/ijepes

Optimal transient droop compensator and PID tuning for load frequency control in hydro power systems

Edimar J. Oliveira *, Leonardo M. Honório, Alexandre H. Anzai, Leonardo W. Oliveira, Exuperry B. Costa

Department of Electrical Energy, Federal University of Juiz de Fora, Brazil

ARTICLE INFO

Article history:
Received 22 November 2013
Received in revised form 8 December 2014
Accepted 24 December 2014
Available online 14 January 2015

Keywords:
Time response specification
Linear and non linear programming
Parameters tuning
Load frequency control

ABSTRACT

This paper presents an optimal method to tune the Proportional, Integral and Derivative (*PID*) controller for a hydraulic turbine coupled with the corresponding Transient Droop Compensator (*TDC*). The proposed methodology is based on the Desired Time Response Specification (DTRS) of the input guide vane servomotor that includes typical rate limiters and gain saturation in power plants. Therefore, the problem consists of adjusting both the parameters of the controller and compensator such as the time response remains close to the specified one. To avoid suboptimal solutions at local minimum points, it is necessary to solve the resulting non linear problem in two steps: (*i*) firstly, solve a linear programming (*LP*) to determine the values of *PID*&*TDC* block using state space representation to match the input and output time responses specifications and (*ii*) determine the final values of the *PID* and *TDC* parameters using the previous results in a new non linear programming. The proposed methodology has presented the advantage of tuning the *PID* coordinated with the *TDC* spending low computational time. The results show that the performance of the method covers a wide range of operating conditions of the system. Comparisons were also made with existing methods in the literature to show the effectiveness of the proposed methodology.

Introduction

One of the most important roles in power system operation is to maintain a continuous energy power supply to the consumers considering quality and security requirements. This objective is achieved by matching the total generation with the total load by using the well known Load Frequency Control (*LFC*) [1], which is responsible to eliminate the frequency deviation and to maintain the active power flow in tie lines in specified values. As the power demanded by the loads change, the system can have several equilibrium points to operate in steady state. The *LFC* has to assure that the system dynamical behaviour, in the transition between the reachable equilibrium points, respect some requirements such as minimum oscillations. To achieve these tasks the Proportional and Integral (*PI*) controller has been widely used and recently the Proportional, Integral and Derivative (*PID*) controller has been studied to improve the results of the *LFC* design [2].

In terms of control techniques for the *LFC* design, the modern optimal control theory allows the calculation of the control system parameters with respect to a given performance criterion as described in [3]. However, its feasibility requires the availability of all the state variables to generate the feedback signal, which is possible if the system state vector is observable from the area measurements [4,5].

The adaptive method is characterized by designing the controllers in order to make them less sensitive to changes in plant parameters and to non-modelled dynamics. The self-tuning controllers are designed to track the operating point of the system updating the controller parameters to achieve an optimum performance [6,7]. Despite the promising results achieved by adaptive controllers, the control algorithms are complicated and require on line system model identification. These efforts seem unrealistic, since it is difficult to achieve them [4].

The Robust control design approaches [8,9] have been tested in the *LFC* design and they allow utilization of physical understanding of power systems and to consider some uncertainties for the synthesis procedure. However, large model size and the elaborate organizational structure of power systems make their direct utilization on these systems too difficult.

Another class of methods for the *LFC* problem is the intelligent approaches using soft computing techniques as well as artificial neural network (*ANN*) [10], fuzzy logic [11–13], genetic algorithm (*GA*) [14,15], particle swarm optimization (*PSO*) [16,17] and bacteria foraging optimization [18].

* Corresponding author. Tel.: +55 32 2102 3440; fax: +55 32 2102 3442.
E-mail address: edimar.oliveira@ufjf.edu.br (E.J. Oliveira).

http://dx.doi.org/10.1016/j.ijepes.2014.12.071
0142-0615/

As well discussed in these references, the *LFC* regulator based on nominal system parameters values is certainly not suitable resulting in a degraded system dynamic performance and sometimes also in the loss of system stability. Thus, the design of a *LFC* with adequate performance requires the tuning of the controller parameters to maintain the frequency even under system condition variations. This problem becomes more important in hydraulic plants because the water starting time parameter (T_W) of the hydro turbine is dependent of the active load condition and also requires a Transient Droop Compensator (*TDC*) to minimize the inverse response characteristic. In addition, the load damping ratio (D) varies with the active load operating point leading the load and machine oscillations to other mode shape.

In the literature, it is possible to find some works that deal with the *LFC* control design considering hydraulic turbines. Ref. [19] considers the hydro turbine dynamics represented by a non minimum phase system and the generation constraints but it not considers the variation of T_W or D with the load. Work [16] used the non minimum phase system representation and it has considered the generation constraint but has not computed the variation of T_W and D with the active load condition. Article [20] had studied the effects of the variation of other parameters of the system to test the robustness of their method, although the parameters considered has not taken in account the variation of T_W and D with the load condition. In [21], the dependence of T_W with the load was considered, but the authors tested only the worst case scenario considering the value of T_W for the maximum load condition.

As already described, the revised works have not been dealing with variation of both parameters T_W and D along the active load condition. It is also common in literature to tune the *PID* controller separately from the transient droop compensator. Seeking for a faster and more efficient methodology for Load Frequency Control (LFC), this paper presents the development of a novel control design approach named Desired Time Response Specification (DTRS) technique based on the input guide vane servomotor (IGVS). This feature results in the following advantages:

(i) the action of the *IGVS* device is specified for having smooth movements without physically impact in the gate. It must be emphasized that this specification is part of the control design process, and the same desired output behaviour may be applied to hydraulic power plants with different capabilities;
(ii) one of the main advantages of the proposed methodology is that the proportional-integral and derivative gains of the *PID* controller, the dash-pot constant and temporary drop of the *TDC* are tuned together. This approach results in a lower stabilization time with reduced impact on *IGVS*;
(iii) the *PID* and *TDC* can be tuned considering different operational point conditions, where both the water time delay (T_W) and load damping (D) vary together in a large range;
(iv) the performance of the *DTRS* method is suitable to operate interconnected power systems, even for abrupt changes in load conditions;
(v) as the *DTRS* design is to specify just the time response of a physical variable, it allows different analysis without deep knowledge in control techniques.

Standard *LFC* design

This section presents the standard *LFC* by using the *PID* controller for a hydro turbine with transient drop compensator (*TDC*). Considering small deviation of the frequency, the turbine and the corresponding speed governor control can be represented as a linearized block diagram. Fig. 1 shows the block diagram of control for an isolated hydro turbine power system.

where:

T_R Dash-pot constant or Reset time in sec;
R_t Temporary droop parameter. R_t can range from 0.01 to 1.2;
R_p Permanent governor speed regulation parameter. R_p is usually equal to 0.05;
Δ_{TC} Represents the output of the transient compensator or the gate servo input (pu-Mw);
T_G Speed governor time constant in sec;
Δ_{GV} Speed valve of the governor (pu-Mw);
$\frac{1}{R}$ Droop characteristic (pu-Mw/Hz);
T_w Water starting time in sec;
Δ_{PL} Active power load perturbation (pu-Mw);
Δ_{PG} Active power generation (pu-Mw);
T_{ps} Power system time constant $T_{ps} = \frac{2 \cdot H}{D \cdot f}, f = 60$ Hz ;
H Machine inertia in sec;
D Loading damping ratio (pu-Mw/Hz);
Δ_{FR} Frequency variation (Hz);
K_{ps} Power system gain (Hz/pu-Mw); $K_{ps} = \frac{1}{D}$;

$\dot{X}_{GV}^{open,\ close}$
The speed valve limiter;

$X_{GV}^{open,\ close}$
The position valve limiter.

A supplementary control action must be used to maintain the nominal value of the frequency. The (*PID*) controller has been investigated for this task. In order to reduce the noise effect the *PID* design can be set as:

$$PID(s) = K_P + \frac{K_I}{s} + \frac{K_D \cdot s}{1 + s \cdot T_D} \tag{1}$$

Where K_P, K_I and K_D are the proportional, integral and derivative gains, respectively. T_D is the derivative filter constant that is used to avoid the noise effect. The design of any supplementary controller for a one machine system is the best place to begin an evaluation of the *PID* controller. After that the global performance is assessed for a two machine system.

As well known, the hydro turbine having a positive zero resulting in a non minimum phase characteristic leading to inverse output of the turbine. For this reason, the system may become unstable for traditional gains. Then, a Transient Droop Compensator (*TDC*) should be included in the speed regulator to improve the stability of the plant. Usually, the *TDC* parameters have been calculated as proposed in Ref. [1]:

$$R_t = [2.3 - 0.15(T_w - 1.0)].\frac{T_w}{2H} \tag{2a}$$

$$T_R = [5.0 - 0.50(T_w - 1.0)].T_w \tag{2b}$$

Proposed *PID* and *TDC* tuning

The proposed formulation has five variables that need to be determined at the same time, K_P, K_I and K_D of the PID controller and T_R and R_t of the transient droop compensator. In this work, the derivative filter constant (T_D) is considered equal to 0.01 as suggested in [22]. For the application of the proposed methodology, the standard representation of Fig. 1 should be redrawn as shown in Fig. 2. It can be seen that the new third order block includes the droop characteristic, *PID* and *TDC*.

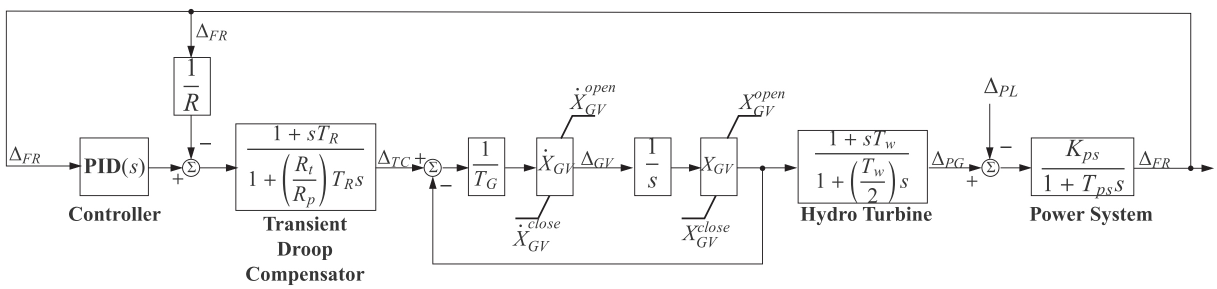

Fig. 1. Block diagram of an isolated system with *PID* controller.

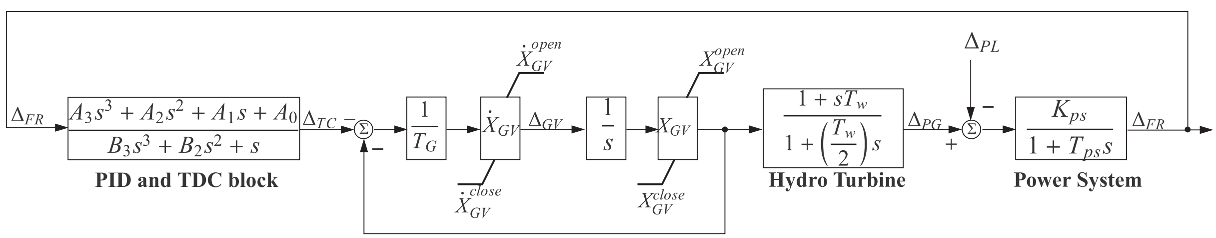

Fig. 2. Modified block diagram of an isolated system.

From comparing the block diagrams of Figs. 1 and 2, the following equations are obtained:

$$A_0 = K_I \quad (3a)$$

$$A_1 = T_D \cdot K_I + K_{P_{Design}} + T_R \cdot K_I \quad (3b)$$

$$A_2 = K_D + T_D \cdot (KP_{Design}) + T_R \cdot K_{P_{Design}} + T_R \cdot T_D \cdot K_I \quad (3c)$$

$$A_3 = T_R \cdot K_D + T_R \cdot T_D \cdot K_{P_{Design}} \quad (3d)$$

$$B_2 = T_D + T_R \cdot \frac{R_t}{R_p} \quad (3e)$$

$$B_3 = T_D \cdot T_R \cdot \frac{R_t}{R_p} \quad (3f)$$

$$K_{P_{Design}} = K_P + \frac{1}{R} \quad (3g)$$

After a disturbance in the system, an increase in the active power load (Δ_{PL}) for example, the output of the transient compensator (Δ_{TC}) varies towards restoring the balance between load and generation. The behaviour of the (Δ_{TC}) should be smooth to avoid saturation in the gate servo movement (Δ_{GV}) of the speed governor. Considering this aspect, the proposed method is based on the specification of the time domain response behaviour of the (Δ_{TC}). For this purpose, the specified (Δ_{TC}) curve is obtained for a basic plant data showed in Appendix A and it can be used to tune both *PID* and *TDC* for any other plant. The process of obtaining (Δ_{TC}) is described in Appendix B.

It can be emphasise that from the specified (Δ_{TC}) the frequency deviation (Δ_{FR}), for any hydro plants, can be easily obtained by using numerical integration resulting in a time domain input of the *PID&TDC* block. In other words, from this point it has the input(Δ_{FR}) and output(Δ_{TC}) signals of the *PID&TDC* block. Consequently, the resulting optimization problem consists of determining the parameters of the third order block that has the designed input and output signals.

To calculate the parameters $A_0, \ldots, A_3, B_2$ and B_3, the third order *PID&TDC* block should be represented by using state-space systems which does not involve derivative terms. The transfer function referred to the *PID&TDC* block is formulated in Eq. (4). By dividing both sides of Eq. (4) by s^3 (5):

$$\Delta_{FR} \cdot (A_3 \cdot s^3 + A_2 \cdot s^2 + A_1 \cdot s + A_0) = \Delta_{TC} \cdot (B_3 \cdot s^3 + B_2 \cdot s^2 + s) \quad (4)$$

$$\Delta_{FR} \cdot \left(A_3 + A_2 \cdot \frac{1}{s} + A_1 \cdot \frac{1}{s^2} + A_0 \cdot \frac{1}{s^3}\right) = \Delta_{TC} \cdot \left(B_3 + B_2 \cdot \frac{1}{s} + \frac{1}{s^2}\right) \quad (5)$$

Rearranging (5) yields in Eq. (6) that can be represented in block diagram as shown in Fig. 3, where Δ_{FR1} is equal to the integration of Δ_{FR} and so on. It can be emphasize that all vectors Δ_{TC} and Δ_{FR} in Eq. (6) have the same numbers of elements as stated in Appendix B.

$$\Delta_{FR} \cdot A_3 + \Delta_{FR1} \cdot A_2 + \Delta_{FR2} \cdot A_1 + \Delta_{FR3} \cdot A_0 - \Delta_{TC1} \cdot B_2 - \Delta_{TC2} = \Delta_{TC} \cdot B_3 \quad (6)$$

After obtaining all vectors of Eq. (6), it is possible to calculate the parameters $A_0 \ldots A_3, B_2$ and B_3 by using the linear programming formulation to take adjustable input and output signals. In this way, the optimization problem can be formulated as shown in Eqs. (7a)–(7f).

$$\min Te_1 = \sum_{k=1}^{m} (R_{L_k} + R_{R_k}) \quad (7a)$$

Subject to :

$$\Delta_{FR_k} \cdot A_3 + \Delta_{FR1_k} \cdot A_2 + \Delta_{FR2_k} \cdot A_1 + \Delta_{FR3_k} \cdot A_0 - \Delta_{TC1_k} \cdot B_2 - \Delta_{TC2_k} - \Delta_{TC_k} \cdot B_3 - R_{L_k} + R_{R_k} = 0 \quad (7b)$$

$$Al_i \leqslant A_i \leqslant Au_i (i = 0, 1, 2, 3) \quad (7c)$$

$$Bl_j \leqslant B_j \leqslant Bu_j (j = 2, 3) \quad (7d)$$

$$R_{L_k} \geqslant 0 \quad (7e)$$

$$R_{R_k} \geqslant 0 \quad (7f)$$

where

- Te_1 Total error of the fitting from linear programming;
- m Number of equality constraints that is equal to the Δ_{TC} length;
- R_R Vector of right residue in the R^m subspace;
- R_L Vector of left residue in the R^m subspace;
- Al_i Lower limit of parameters A_i;
- Au_i Upper limit of parameters A_i;
- Bl_j Lower limit of parameters B_j;
- Bu_j Upper limit of parameters B_j.

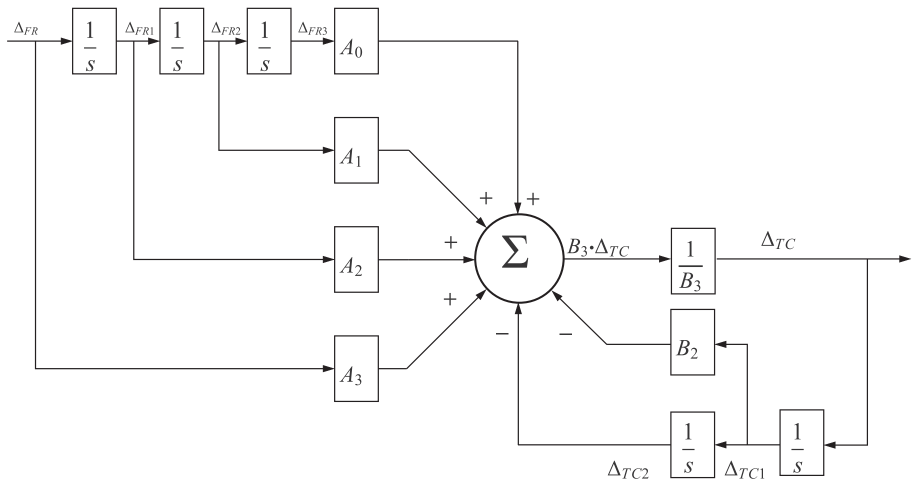

Fig. 3. *PID&TDC* block in state-space representation.

The lower and the upper limits of A_i and B_j are obtained by using Eqs. (3a)–(3f) considering the minimum and maximum values of variables from *PID* and *TDC*, respectively. These values will be given hereafter. The minimum value of the objective function corresponds to the best fitting of all A_i and B_j. It is important to mention that this problem is a linear programming (*LP*), so its solution requires low computational effort. This paper has been used the MATLAB© optimization toolbox based on a linear interior point solver [23], which is a variant of the Mehrotra's predictor–corrector algorithm [24].

Once A_i and B_j have been determined, the values of the *PID* controller (K_P, K_I and K_D) and the compensator (R_t and T_R) can be calculated by Eqs. (3a)–(3g). However, the analytical solution to this system may not be obtained within the range of the variables because the parameters A_i and B_j are an approximation. Therefore, the *PID* and *TDC* variables can be calculated by solving a Non Linear Programming (*NLP*) problem related with the least square deviation that have no equality constraints as shown in Eqs. (8a)–(8f).

$$\min Te_2 = \sum_{n=1}^{6} (DEV_n)^2 \tag{8a}$$

Subject to :

$$0 \leqslant K_{P_{Design}} \leqslant 5.0 \tag{8b}$$

$$0 \leqslant K_I \leqslant 5.0 \tag{8c}$$

$$0 \leqslant K_D \leqslant 5.0 \tag{8d}$$

$$0.001 \leqslant T_R \leqslant 9.0 \tag{8e}$$

$$0.01 \leqslant R_t \leqslant 1.2 \tag{8f}$$

where Te_2 is the total error of the fitting from non linear programming. In addition, the minimum and maximum values of the *PID* and *TDC* variables come from their usual limits and:

$$DEV_1 = A_0 - K_I \tag{9a}$$

$$DEV_2 = A_1 - (T_D \cdot K_I + K_{P_{Design}} + T_R \cdot K_I) \tag{9b}$$

$$DEV_3 = A_2 - (K_D + T_D \cdot K_{P_{Design}} + T_R \cdot K_{P_{Design}} + T_R \cdot T_D \cdot K_I) \tag{9c}$$

$$DEV_4 = A_3 - (T_R \cdot K_D + T_R \cdot T_D \cdot K_{P_{Design}}) \tag{9d}$$

$$DEV_5 = B_2 - \left(T_D + T_R \cdot \frac{R_t}{R_p}\right) \tag{9e}$$

$$DEV_6 = B_3 - \left(T_D \cdot T_R \cdot \frac{R_t}{R_p}\right) \tag{9f}$$

As this problem is a non linear programming with only five optimization variables (K_P, K_I, K_D, R_t and T_R) and without equality constraints, its solution can be easily found with small computational effort. This paper has been used the MATLAB© optimization toolbox based on a non linear interior point algorithm [25]. The solution of this optimization problem can found the optimal *PID* and *TDC* parameters that are able to operate the hydro plant within the specified devices conditions.

In addition, it is recognized that both water starting time of the hydro turbine (T_W) and the active load damping (D) vary according to the active power load. In this sense, it becomes necessary to adjust the *PID* and *TDC* to ensure proper operation of the system for multiple Operating Condition (*oc*). In the proposed methodology, this is accomplished through three steps:

(i) Solve the linear optimization problem (*LP*) that have been described in (7a)–(7f) to find both A_i^{oc} and B_j^{oc} parameters for each operating condition. This step uses the unique specified (Δ_{TC}) and corresponding (Δ_{FR}^{oc}) for each operating condition;
(ii) For each pair (A_i^{oc}, B_j^{oc}), simulate the system by using numerical integrations and get the new input (Δ_{FR}^{oc}) and output (Δ_{TC}^{oc}) signals for all operating points;
(iii) Solve the Extend Linear Programming (*ELP*) as outlined in Eqs. (10a)–(10f) to find the unique A_i and B_j capable to match all the input and output signals. It should be reinforced that it is not necessary to compute all points of the input (Δ_{FR}^{oc}) and output (Δ_{TC}^{oc}) signals to take the solution of *LP* (10a)–(10f) being enough to consider only two-thirds of the corresponding part of the tail of the curves.

$$\min \quad Te_3 = \sum_{oc=1}^{n_{oc}} \sum_{k=1}^{m} \left(R_{L_k}^{oc} + R_{R_k}^{oc}\right) \tag{10a}$$

Subject to :

$$\Delta_{FR_k}^{oc} \cdot A_3 + \Delta_{FR1_k}^{oc} \cdot A_2 + \Delta_{FR2_k}^{oc} \cdot A_1 + \Delta_{FR3_k}^{oc} \cdot A_0 - \Delta_{TC1_k}^{oc} \cdot B_2 - \Delta_{TC2_k}^{oc} - \Delta_{TC_k}^{oc} \cdot B_3 - R_{L_k}^{oc} + R_{R_k}^{oc} = 0 \tag{10b}$$

$$Al_i \leqslant A_i \leqslant Au_i (i = 0, 1, 2, 3) \tag{10c}$$

$$Bl_j \leqslant B_j \leqslant Bu_j (j = 2, 3) \tag{10d}$$

$$R_{L_k} \geqslant 0 \tag{10e}$$

$$R_{R_k} \geqslant 0 \tag{10f}$$

In this formulation n_{oc} represents the number of the operation condition. It should be stressed that using the values of A_i and B_j obtained from the solution of problem (10a)–(10f), the final values of the *PID* and *TDC* parameters can be taken by solving the *NLP*

Eqs. (8a)–(8f). These values are adjusted to operate the power hydro plants in many active power loads conditions.

The *LFC* results for single machine power systems

This section presents an analysis considering a single machine power plant to explain the proposed *DTRS* approach and verify its robustness related to simultaneous parameter variations (T_w and D). The results are compared with the Maximum Peak Resonance Specification (MPRS) based method presented in [21] where the goal was just the PID tuning.

Case-A: Tutorial analysis

In this tutorial case, the goal is to demonstrate the *DTRS* technique in a well-known power plant. The *DTRS* uses the Time Response Specification (*TRS*) of the input guide vane servomotor (Δ_{TC}) for tuning both the *PID* and *TDC*. The power plant data and the process of obtaining the *TRS* are shown, respectively in Appendices A and B.

From the specified Δ_{TC} showed in Fig. 19 and using numerical integration based on trapezoidal approximation, the corresponding Δ_{FR} is obtained as shown in Fig. 20. Δ_{FR} and Δ_{TC} are the coefficients of A_3 and B_3 in Eq. (7b), respectively. The corresponding coefficients of A_2, A_1 and A_0 are shown in semi-log scale in Fig. 4 as well as the coefficients Δ_{TC1} and Δ_{TC2} are displayed in Fig. 5. From this point the linear program can be solved to find the optimal values of A_i and B_j that minimize (7a).

Table 1 shows the optimal values of A_i and B_j that have matched the input Δ_{FR} and the output Δ_{TC} signals. As expected in this case, the Total error (Te_1) of the fitting is almost zero because in this study the same plant is matched.

From the values of A_i and B_j the proposed approach is able to solve the non linear optimization problem (8a)–(8f) to find the adjustable values of the *PID* controller and *TDC* compensator as show in Table 2. In this case the Total error (Te_2) is equal to 1.43×10^{-6}. As the minimal value of the time reset (T_R) is equal to 0.001, the optimization has found ($T_R = 0.0011$) and ($R_t = 27.7715\%$) instead the null values from the original plant.

Case-B: Time simulation equal to 100 s

Another simulation is carried out using the same hydro plant data showed in Appendix A. In this case the purpose is to determine the new *TDC* and *PID* to reduce the initial open speed governor gate. As described in Appendix A, it can be obtained by using

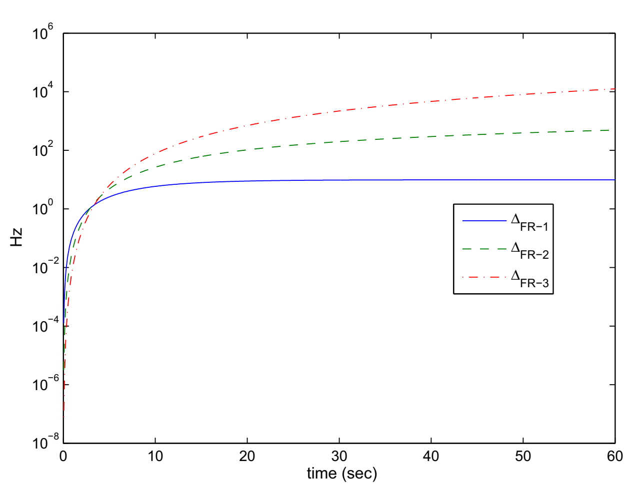

Fig. 4. Δ_{FR1}, Δ_{FR2} and Δ_{FR3} coefficients.

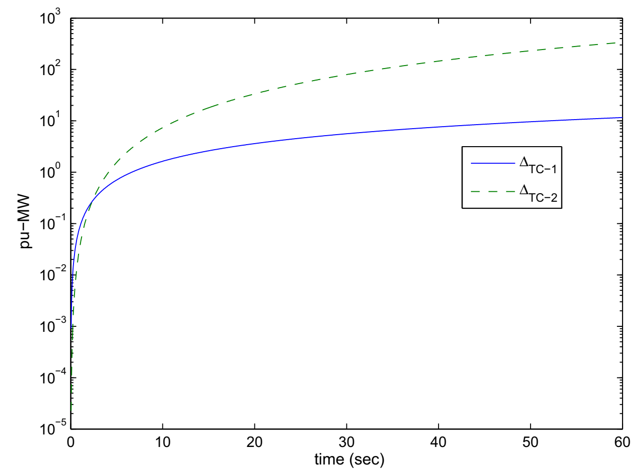

Fig. 5. Δ_{TC1} and Δ_{TC2} coefficients.

Table 1
Solution of problem (7a)–(7f).

Te_1	A_3	A_2	A_1	A_0	B_2	B_3
1.4×10^{-9}	1.5×10^{-3}	0.2526	0.1642	0.0203	0.0158	$5.82.10^{-5}$

Table 2
Solution of problem (8a)–(8f).

Te_2	K_I	$K_{P_{Design}}$	K_D	R_t (%)	T_R
1.43×10^{-6}	0.0203	0.1639	0.2508	27.7715	0.0011

the same Δ_{TC} considering simulation time $T = 100$ seconds, see Fig. 21. In other words, the hydro plant will have more time to accommodate initial variations, reducing the impact of regulator actions and increasing stabilization. Following the same steps previously stated, the proposed approach solve the *LP* (7a)–(7f) and the *NLP* (8a)–(8f) to find the new parameters of *PID* and *TDC*, as shown in Table 3. The errors are close to zero and the parameters of *PID* and *TDC* were modified resulting in a new behaviour belong the time.

Fig. 6 shows the initial output of Δ_{TC} for both *DTRS* and *MPRS* methods. It can be observed that adding the Transient Droop Compensator (TDC) reduces the action of Δ_{TC} as well as the initial behaviour of the speed governor gate as shown in Fig. 7.

Another advantage of the adjustment of both *PID* and *TDC* can be seen in Fig. 8.When *DTRS* is used, the variation of Δ_{PG} presents a reduction in the inverse response of the hydro turbine. The inverse-response characteristic associated with 20 MW raise in active power load lead to a Δ_{PG} sank 14 MW for *MPRS* and 12 MW for *DTRS*. This 2 MW represents an energy saving of 14.28% between two methods. Even the *DTRS* has reduced the initial controller's action the result of steady state was not degraded as shown in Fig. 9.

Case-C: Simulation results for different hydro power plants

This case study shows the application of the proposed methodology to regulate a hydraulic plant that has the Nominal Power

Table 3
New adjustable *PID* and TDC for *NP* = 1000 MW: Case-B.

Te_1	Te_2	K_I	$K_{P_{Design}}$	K_D	R_t (%)	T_R
1×10^{-5}	1×10^{-12}	0.0184	0.1494	0.2598	5.8304	0.9754

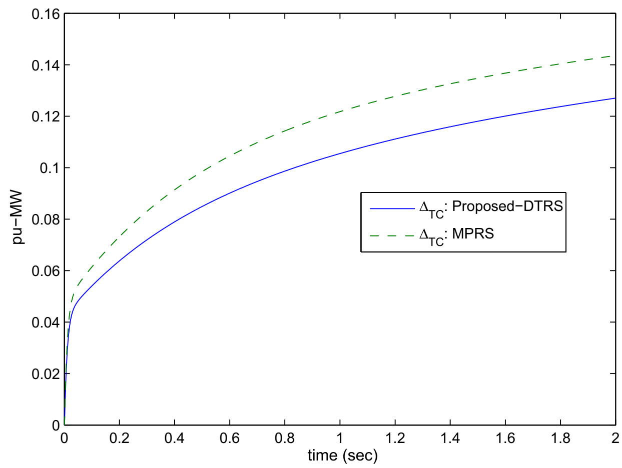

Fig. 6. Initial action of $\Delta_{TC's}$.

(NP) equal to 350 MW. It can be stressed that this (NP) is too different of the basic (1000 MW) power plant used as standard in the Appendix B. The parameters are as follows:

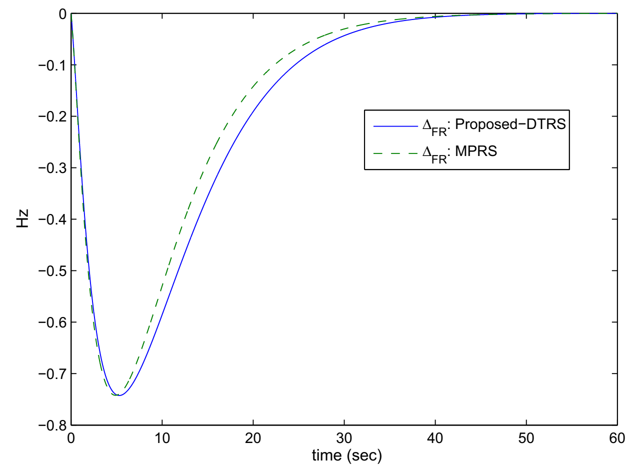

Fig. 9. Total Δ_{FR} oscillations.

Being the active power load (PL) a percentage of NP, the frequency (f) equal to 60 Hz and the limiter values the same of the standard, these parameters referred in the base power equal to

System	350 MW:	$T_G = 0.5$	$T_W = 3.0$	$R_p = 0.05$	$T_D = 0.01$	
		$H = 5$	$D\% = 1$	$NP = 350$ MW	$PL = 0.75 \cdot NP$	$\Delta_{PL} = 0.02 \cdot NP$

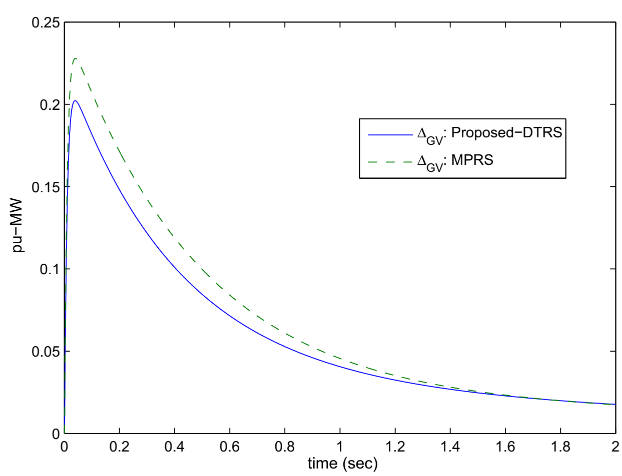

Fig. 7. Initial behaviour of speed governor gate.

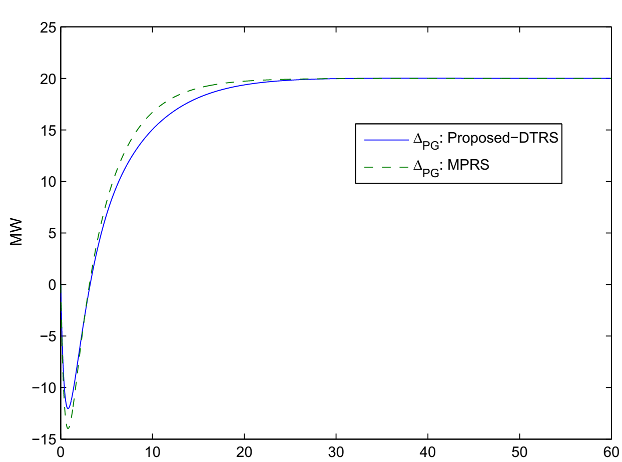

Fig. 8. Total Δ_{PG} oscillations.

(BP) = 100 MV A results:

$$\begin{aligned}
&D = D\% \cdot \frac{PL}{BP \cdot f} = 1.\ \frac{0.75 \cdot 350}{100 \cdot 60} = 0.0437 \text{ pu-MW/Hz} \\
&H = H \cdot \frac{NP}{BP} = 5 \cdot \frac{350}{100} = 17.5 \text{ s} \\
&K_{ps} = \frac{1}{D} = 22.8833 \text{ Hz/pu-MW} \\
&T_{ps} = \frac{2H}{D \cdot f} = \frac{35}{0.0437 \cdot 60} = 13.33 \text{ s} \\
&\frac{1}{R} = \frac{1}{R_p} \cdot \frac{NP}{BP \cdot f} = 20 \cdot \frac{350}{100 \cdot 60} = 1.1667 \text{ pu-MW/Hz} \\
&\Delta PL = 0.02 \cdot \frac{NP}{BP} = 0.07 \text{ pu} - \text{MW}
\end{aligned} \tag{11}$$

$$\dot{X}_{GV}^{open} = 0.16 \cdot \frac{350}{100} = 0.56; \quad \dot{X}_{GV}^{close} = 0.16 \cdot \frac{350}{100} = 0.56;$$
$$X_{GV}^{open} = 0.1 \cdot \frac{350}{100} = 0.35; \quad X_{GV}^{close} = 0.1 \cdot \frac{350}{100} = 0.35.$$

To use the proposed approach, it is necessary to specify Δ_{TC} property to respond to 0.07 pu-MW in load variation ($\Delta_{PL} = 0.07$ pu-MW). In this case, the specified Δ_{TC} is obtained by simulating the basic plant of Appendix A considering the load variation equal to a 0.07 pu-MW and T = 60 s. The specified Δ_{TC} is similar to that showed in Fig. 19 and it is obtained by simply replacing the (y) axis values. Using this just Δ_{TC} and numerical integration, the corresponding Δ_{FR} for this 350 MW power plant is obtained as shown in Fig. 10. Therefore, using Δ_{FR} as input and Δ_{TC} as output of the *PID&TDC* block, the *DTRS* technique find a set of tuned values for the *PID* and *TDC* to control the 350 MW power plant property.

To achieve this goal the problems (7a)–(7f), (8b)–(8f) *PID* and *TDC* that is able to match Δ_{FR} and Δ_{TC} curves. Table 4 shows the results for this simulation whose errors are close to zero and the parameters of *PID* and *TDC* were modified according to the new power plant characteristic. Fig. 11 shows the Δ_{TC} deviation for both the specified(standard) and 350 MW power plants. These results show that the proposed approach was able to tune both the *PID*

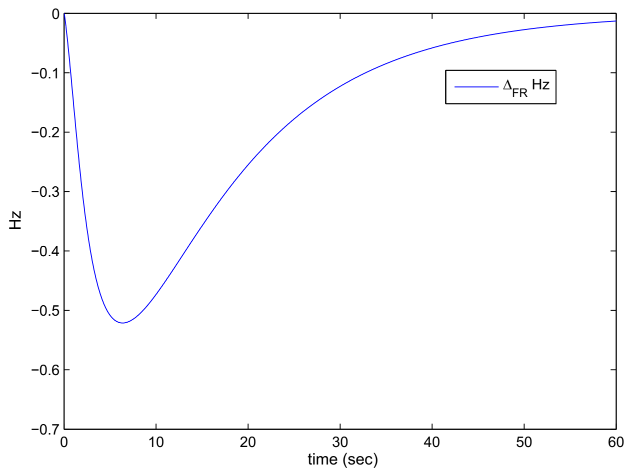

Fig. 10. Corresponding Δ_{FR} – The *PID&TDC* block input of the 350 MW power plant.

Table 4
PID and *TDC* tuning for *NP* = 350 MW: Case-C.

Te_1	Te_2	K_I	$K_{P_{Design}}$	K_D	R_t (%)	T_R
3.0×10^{-3}	2.0×10^{-10}	0.0063	0.1309	0.6357	20.6099	1.8566

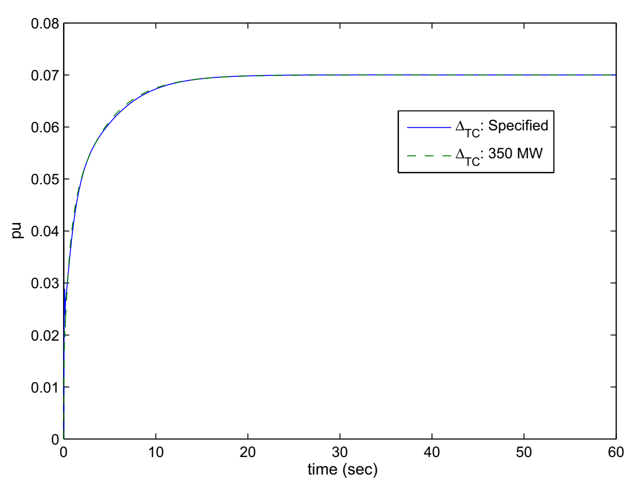

Fig. 11. Δ_{TC} for the hydro 350 MW power plant.

and *TDC* by using a different power plant. In other words, any plant can be adjusted to follow the behaviour of another known plant.

Sensitivity analysis

It is known that the water starting time (T_w) and the load damping (D) change along with active power load variation, which may lead to a performance degradation in the plant. The variation of parameter D affect the power system gain (K_{ps}), which can cause degradation in the stead state response. In addition, the variation of the parameter T_w changes the position of the positive zero influencing dynamic behaviour. To avoid this situation, *PID* and *TDC* should be tuned considering various operating point condition (oc). Therefore, another simulation is carried out in which the active power load (P_L) varies from 90% to 65% of the Nominal Power (*NP*) capacity of the 350 MW power plant. These operating points represent the heavy and medium load, respectively. This paper adopts the variation of T_w according to the P_L condition as shown in Table 5. In addition, Table 5 also presents the corresponding values of D, K_{ps} and T_{ps}. It can be observed that both T_w and D decrease as well as *PL*.

Table 5
Operation conditions.

OC	$PL = \%NP$	T_w	D(pu-MW/Hz)	$K_{ps} = 1/D$	T_{ps}
1	90	5.0	0.0525	19.0476	11.1111
2	80	4.0	0.0467	21.4286	12.5000
3	75	3.0	0.0437	22.8833	13.3333
4	70	2.0	0.0408	24.4898	14.2857
5	65	1.0	0.0379	26.3736	15.3846

In Case-C stated before, the 350 MW power plant has been tuned for the operation condition number 3. Therefore, in this sensitivity analysis, the proposed methodology uses this operating point as well as standard condition Δ_{TC} as shown in Fig. 11. So the Δ_{TC} responds to 0.07 pu-MW in load variation ($\Delta_{PL} = 0.07$ pu-MW) for all operating conditions.

After obtaining the corresponding (Δ_{FR}^{oc}) from Δ_{TC}, it is necessary to solve the optimization problems (7a)–(7f), (8b)–(8f) for each operating point stated in Table 5, resulting in adjustable *PID* and *TDC* as showed in Table 6.

Although each setting is the best for its operating point, it is necessary to determine a unique *PID* and *TDC* setting to control this hydro plant in all operation conditions. The proposed problems (10a)–(10f), (8b)–(8f) are adequate to treat this issue and the solution brings the adjusted *PID* controller and *TDC* compensator, as shown in Table 7. The unique *PID* and *TDC* tuning has tested for all operation condition of Table 5 resulting in suitable performance. In addition, it was tested in extreme operation points considering light and heavy ($oc = 1$) active power load. For light load, $T_w = 0.1$ s and *PL* = 10% of *NP* were adopted. Fig. 12 shows the frequency deviations corresponding to the both light and heavy active power loads where the behaviour can be considered suitable for these extreme operating points.

Computational aspects

As stated before, the proposed methodology has broken the *PID* and *TDC* tuning down into two optimization problems to avoid a large non linear quadratic problem. The first problem has spent low computational time because it has been written as a linear program and solved by using the Interior Point Method of the MATLAB© ToolBox called linprog. The advantage of using linear programming is related to a convex region close to a viable operating point. So, even under about a thousand linear constraints, the problems (7a)–(7f), (10b)–(10f) spend about two seconds to find the solution.

The second optimization problem is a non linear programming, but it has only five variables without constraints resulting in an easily problem to be solved that has a negligible computational time.

Table 6
PID and *TDC* tuning for each operation conditions.

OC	K_D	K_I	$K_{P_{Design}}$	R_t (%)	T_R (s)
1	0.8599	0.0053	0.1361	27.4789	2.7056
2	0.7491	0.0055	0.1287	24.1752	2.2753
3	0.6357	0.0063	0.1309	20.6099	1.8566
4	0.5143	0.0075	0.1414	16.7077	1.4150
5	0.4048	0.0096	0.1707	15.3075	0.6823

Table 7
Unique *PID* and *TDC* tuning for all operation conditions.

K_D	K_I	$K_{P_{Design}}$	R_t (%)	T_R
0.6815	0.0059	0.1277	22.0624	2.0651

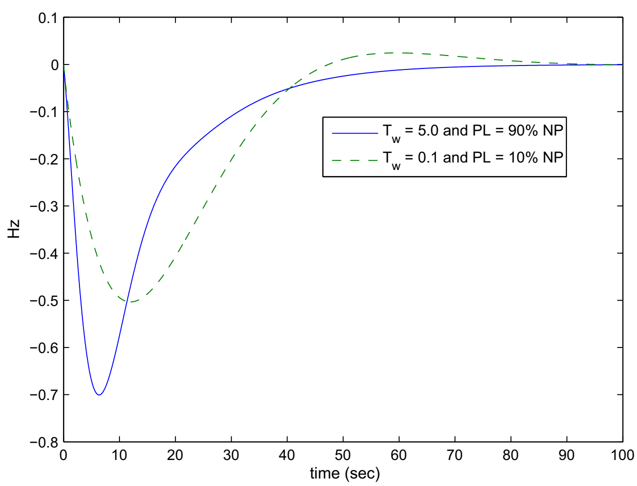

Fig. 12. Δ_{FR} for extreme operation condition.

The *LFC* results for two-area power systems

Another simulation was carried out considering a two-area interconnected power system to test the tie line performance when the *DTRS* technique has been used to tune *PID* and *TDC*. The results will be compared with the *MPRS* method. The two systems are the same ones tested before: the 1000 MW and the 350 MW systems refereed in the base power *BP* = 100 MV A. A set of perturbations $\Delta_{PL_{1000}} = +100$ MW and $\Delta_{PL_{350}} = -35$ MW are considered.

The *PID* and *TDC* parameters for the 350 MW system are showed in Table 4 and they are used for both *DTRS* and *MPRS* methods. For the 1000 MW system, the *DTRS* adopts the *PID* and *TDC* as shown in Table 3 and *MPRS* uses the *PID* parameters described in Appendix A.

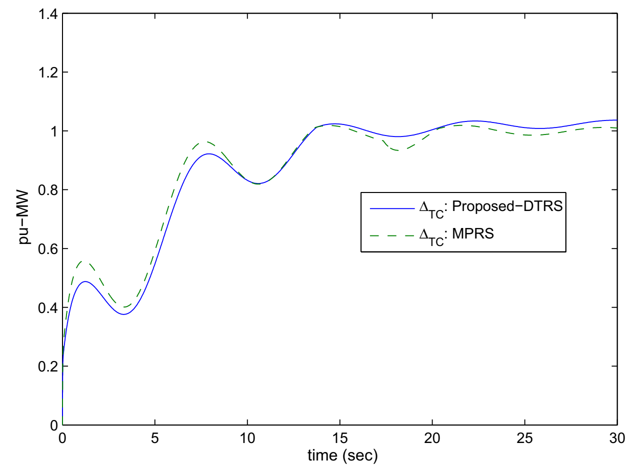

Fig. 14. Initial behaviour of $\Delta_{TC's}$.

To remove the area control error (*ACE*) after the disturbance, this work adopted the same control strategy proposed in Ref. [21]. In this case the frequency bias (*B*) are setted equal to one for both systems and the tie line deviation (ΔP_{tie}) receives an integral action and it is included in the summation after the *PID* controller by using the tie line feedback gain (g_1) equal to 0.1 for the 1000 MW system. For the 350 MW system, the present paper proposes the tie line feedback gain (g_2) equal to 0.035 corresponding to its proportional capacity. Fig. 13 shows the block diagram for these interconnected systems, where the 1000 MW and the 350 MW power plants are represented by system 1 and 2 respectively. The tie line parameter (T_{12}) is considered equal to 0.15.

The simulation results show the effectiveness of *DTRS* technique for both dynamic and steady state condition. Results will be presented only for the system 1 due to the fact that it is controlled by both DTRS and MPRS, providing a suitable comparison case

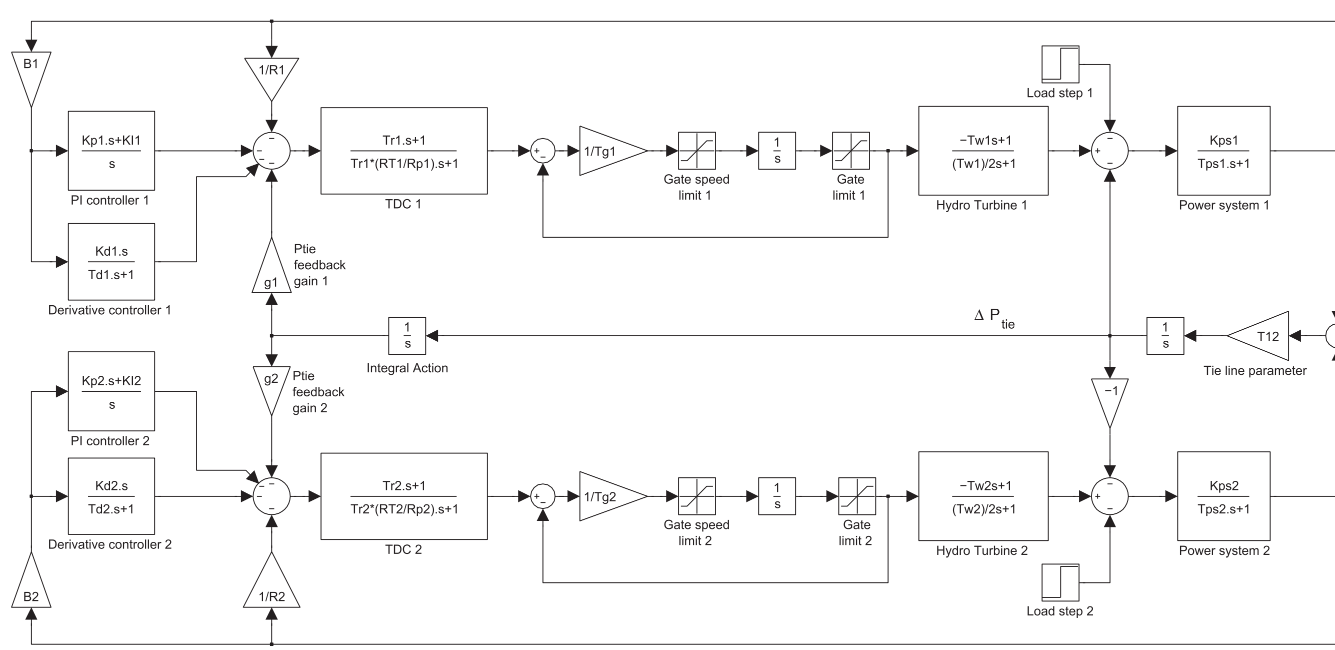

Fig. 13. Block diagram for two machine system.

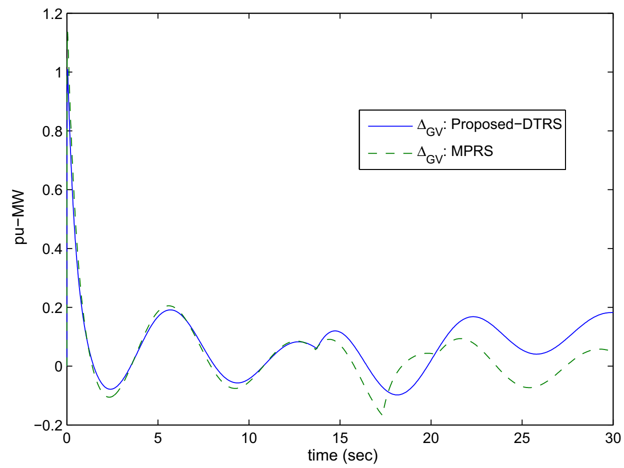

Fig. 15. Initial behaviour of speed governor gate.

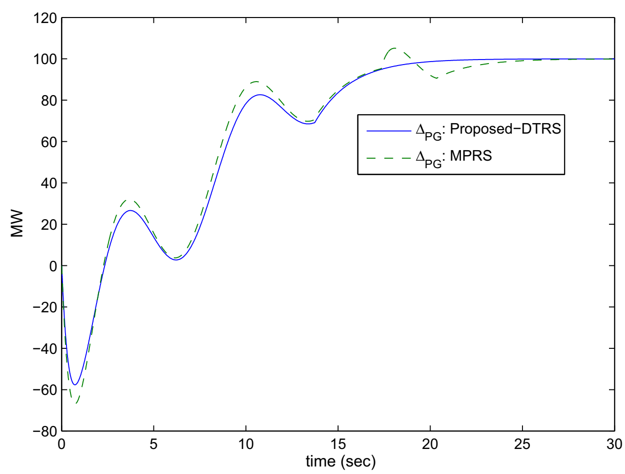

Fig. 16. Initial Δ_{PG} deviation.

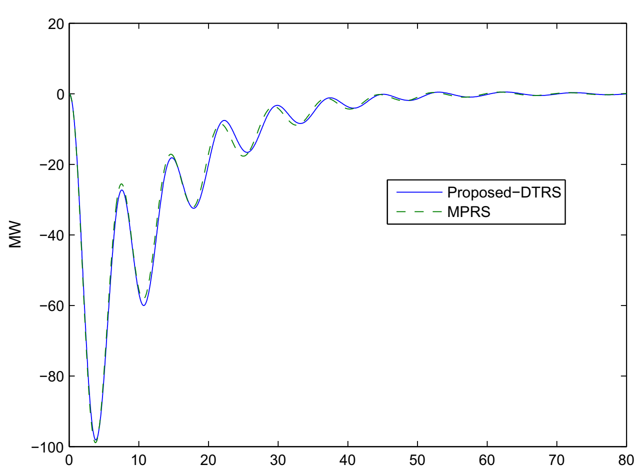

Fig. 17. Tie line power oscillation after the disturbance (ΔP_{tie12}).

scenario. Fig. 14 shows the action of Δ_{TC} during the first 30 s simulation. The *PID* and Transient Droop Compensator (TDC) evaluated in *DTRS* reduces the impact and oscillations of the Δ_{TC} when compared with *MPRS*. These conditions results in smoother speed governor gate variation as shown in Fig. 15. Considering that these variables represents a mechanical system, any reduction of impact and oscillations are attractive because they increase the equipments lifetime.

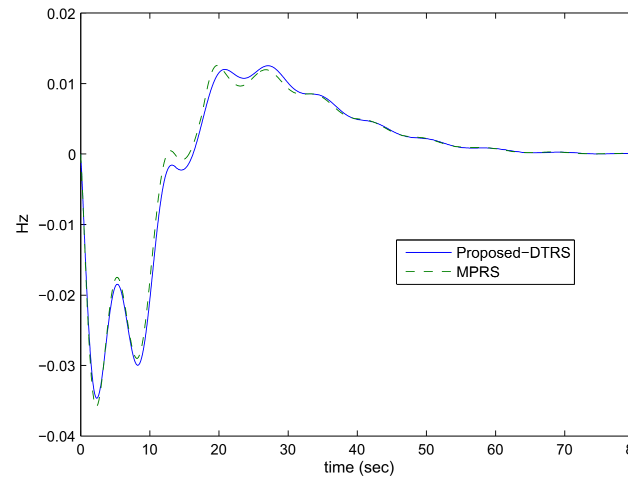

Fig. 18. Frequency oscillation after the disturbance.

Fig. 16 shows the variation of Δ_{PG}. The inverse response of the hydraulic turbine was reduced from 67 MW in *MPRS* to 57 MW in the *DTRS* approach. In this case, the *DTRS* was able to prevent 10 MW of inverse response and it also reduced the hydraulic turbine power oscillations.

Fig. 17 presents the tie line oscillation after the disturbances (ΔP_{tie12}) for both tuning *DTRS* and *MPRS*. As the load increases in system 1, the ΔP_{tie} is negative until it recovers the load-generation equilibrium.

As shown in Fig. 18, the frequency deviations were minimized with a maximum deviation of 0.035 Hz. Although the results were almost the same, the oscillations have been lower for *DTRS*technique. These results show that the proposed *PID* and *TDC* tuning is also suitable to control interconnected power systems without frequency mismatches and tie line oscillations in steady state.

Concluding remarks

This paper presented a new approach for tuning both *PID* controller and Transient Droop Compensator (TDC) in Load Frequency Control (LFC) of hydro turbine problems. The proposed methodology is based on a Desire Time Response Specification (DTRS) of the Input Guide Vane Servomotor (IGVS). From the results presented in this paper, the following main aspects can be emphasized:

– the proposed *IGVS* specification yielded satisfactory performance for the analysis of two hydraulic plants considering different operating points where both water time delay (T_W) and load damping (D) varied together in a large range;
– the *IGVS* device response always presented a smooth action, reducing the impact on the gate and, therefore, improving its lifetime;
– reduced oscillations and stabilization time were obtained because the proportional-integral and derivative gains of the *PID* controller, the dash-pot constant, and the temporary droop of the *TDC* were tuned together;
– even with abrupt changes in active power load, the performance of the *DTRS* method presented suitable operative conditions in an interconnected system for both dynamic and steady state;
– the proposed *DTRS* approach spent low computational time to tuning both *PID* and *TDC*.

It is also important to mention that the proposed method was compared with the *MPRS* approach and it was demonstrated that the *DPRS*, with the same project controller design, covered a wider range of operating conditions including interconnected power systems.

As discussed in the paper, the proposed methodology presented very good qualitative and quantitative results. Besides, its design approach, namely to specify a time response output, is easily understood for field engineers.

Acknowledgments

The authors would like to thank INERGE, CAPES/PNPD, CNPq and FAPEMIG for the financial support.

Appendix A

The typical hydro power plant proposed in Ref. [1] is used in this paper to show the main aspects of the proposed technique. In addition, the *PID* controller described in Ref. [21], where the transient droop compensator was not considered, is used to compare the results. The parameters are given in MVA base equal to the Nominal Power ($NP = 1000$ MW) and the Power Load (PL) demand was considered equal to NP. The data are as follows:

$T_G = 0.2 \quad T_W = 4.0 \quad 2H = 6 \quad D\% = 1 \quad R_p = 0.05$

$1/R = 20 \quad \Delta_{PL} = 0.02pu$

The *PID* controller proposed in [21] are:

$T_D = 0.01 \quad K_I = 0.122 \quad K_D = 1.5 \quad KP_{Design} = 0.983$

$R_t(\%) = 0 \quad T_R = 0$

The limiter values are [1,21,26]:

$\dot{X}_{GV}^{open} = 0.16 \quad \dot{X}_{GV}^{close} = 0.16 \quad X_{GV}^{open} = 0.1 \quad X_{GV}^{close} = 0.1$

These parameters referred in Base Power (BP) equal to 100 MV A results:

$$D = D\% \cdot \frac{PL}{BP \cdot f} = 1 \cdot \frac{1000}{100 \cdot 60} = 0.1667; \quad H = H \cdot \frac{NP}{BP} = 3 \cdot \frac{1000}{100} = 30;$$

$$K_{ps} = \frac{1}{D} = \frac{100 \cdot 60}{1000} = 6.0; \quad T_{ps} = \frac{2H}{D \cdot f} = \frac{60}{0.1667 \cdot 60} = 6.0;$$

$$\frac{1}{R} = \frac{1}{R_p} \cdot \frac{NP}{BP \cdot f} = 20 \cdot \frac{1000}{100 \cdot 60} = 3.3333; \quad \Delta PL = 0.02 \cdot \frac{NP}{BP} = 0.2\,\text{pu};$$

$$K_{PID} = K_{PID} \cdot \frac{NP}{BP \cdot f} \quad \text{Resulting in}: \quad K_I = 0.0203 \quad K_D = 0.2500$$

$$\text{and } KP_{Design} = 0.1638$$

$$\dot{X}_{GV}^{open} = 0.16 \cdot \frac{1000}{100} = 1.6; \quad \dot{X}_{GV}^{close} = 0.16 \cdot \frac{1000}{100} = 1.6;$$

$$X_{GV}^{open} = 0.1 \cdot \frac{1000}{100} = 1; \quad X_{GV}^{close} = 0.1 \cdot \frac{1000}{100} = 1.$$

Appendix B

This appendix shows the process to calculate the basic (Δ_{TC}) in time domain. This paper has chosen the trapezoidal integration methods where the step h is considered equal to $h = 0.05$ and the time of simulation $T = 60$ s were adopted. Using the system data and *PID* controller described above, the basic (Δ_{TC}) vector will have 1200 elements. Fig. 19 shows the basic (Δ_{TC}) behaviour that will be used to tune any hydro plants discussed in this paper.

Fig. 20 shows the frequency deviation (Δ_{FR}) in Hz for this hydro plants. It can be emphasized that only (Δ_{TC}) curve will be specified in the proposed approach. In other words, using the same (Δ_{TC}) for different hydro plants, different (Δ_{FR}) can be obtained.

It should be emphasized that the basic curve (Δ_{TC}) can be rearranged to simulate both different simulation times and variations in an active power load. Supposing for example the simulation time is equal to $T = 100$ s and $\Delta_{PL} = 0.2$ pu, then the new basic (Δ_{TC}) is obtained from time simulating of basic plant considering $T = 60$ s,$\Delta_{PL} = 0.2$ pu and $h = 0.05^{*}60/100 = 0.03$ leading to 1800 elements. Fig. 21 displays the 1800 elements of Δ_{TC} for $T = 100$ s

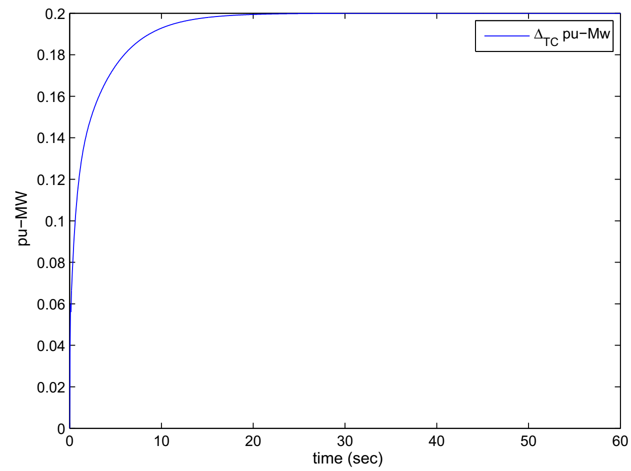

Fig. 19. Specified Δ_{TC} deviation.

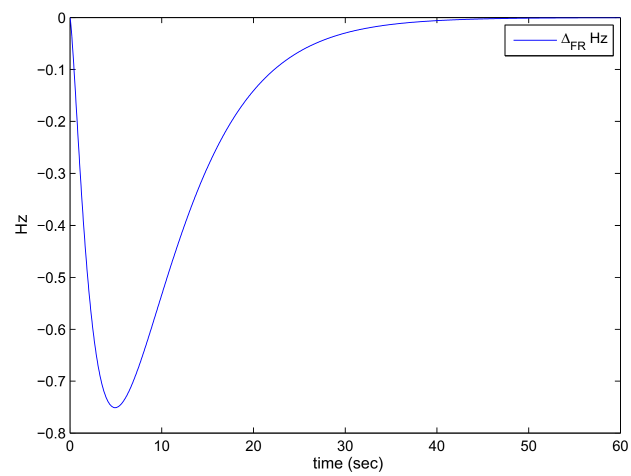

Fig. 20. Corresponding Δ_{FR} deviation.

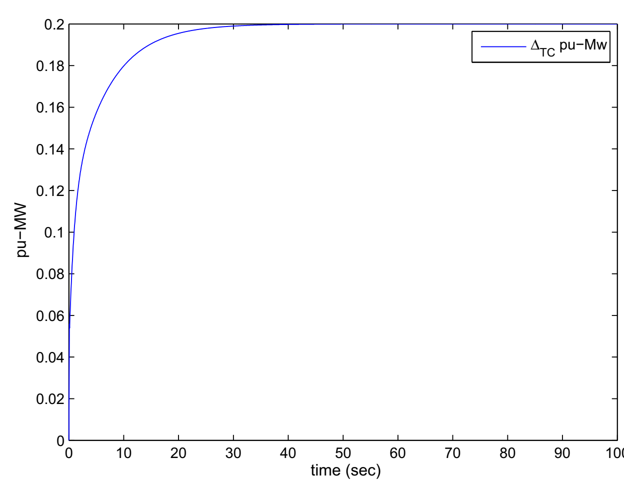

Fig. 21. Δ_{TC} deviation for $T = 100$.

which has the same mode shape of Fig. 19 in a different time simulation.

References

[1] Kundur P. Power system stability and control. McGraw-Hill Inc; 1994.

[2] Pandey SK, Mohanty SR, Kishor N. A literature survey on load-frequency control for conventional and distribution generation power systems. Renew Sust Energy Rev 2013;25(0):318–34. http://dx.doi.org/10.1016/j.rser.2013.04.029. <http://www.sciencedirect.com/science/article/pii/S1364032113002815>.

[3] Velusami K, Ramar S. Design of observer-based decentralized load-frequency controllers for interconnected power systems. Int J Power Energy Syst 1997;17(2):152–60. iSSN: 1078-3466.

[4] Shayeghi H, Shayanfar H, Jalili A. Load frequency control strategies: a state-of-the-art survey for the researcher. Energy Convers Manage 2009;50(2):344–53. <http://www.sciencedirect.com/science/article/pii/S0196890408003567>.

[5] Hasan N, Ibraheem, Kumar P, Nizamuddin. Sub-optimal automatic generation control of interconnected power system using constrained feedback control strategy. Int J Electr Power Energy Syst 2012;43(1):295–303. http://dx.doi.org/10.1016/j.ijepes.2012.04.039. <http://www.sciencedirect.com/science/article/pii/S0142061512001664>.

[6] Lee K, Yee H, Teo C. Self-tuning algorithm for automatic generation control in an interconnected power system. Electric Power Syst Res 1991;20(2):157–65. <http://www.sciencedirect.com/science/article/pii/037877969190060Z>.

[7] Rubaai A, Udo V. Self-tuning load frequency control: multilevel adaptive approach. IEE Proc–Gener Transm Distrib 1994;141(4):285–90. <http://digital-library.theiet.org/content/journals/10.1049/ip-gtd19949964>.

[8] Bevrani H, Mitani Y, Tsuji K. Robust decentralised load-frequency control using an iterative linear matrix inequalities algorithm. IEE Proc–Gener Transm Distrib 2004;151(3):347. http://dx.doi.org/10.1049/ip-gtd:20040493. http://dx.doi.org/10.1049/ip-gtd:2004.04.93.

[9] Koisap C, Kaitwanidvilai S. A novel robust load frequency controller for a two area interconnected power system using lmi and compact genetic algorithms. In: TENCON 2009 – 2009 IEEE region 10 conference; 2009. p. 1–6. http://dx.doi.org/10.1109/TENCON.2009.5395937.

[10] Mishra P, Mishra S, Nanda J, Sajith K. Multilayer perceptron neural network (mlpnn) controller for automatic generation control of multiarea thermal system. In: North American Power Symposium (NAPS), 2011; 2011. p. 1–7. http://dx.doi.org/10.1109/NAPS.2011.6024887.

[11] Masiala M, Ghribi M, Kaddouri A. An adaptive fuzzy controller gain scheduling for power system load-frequency control. In: 2004 IEEE International conference on industrial technology, 2004. IEEE ICIT '04, vol. 3, 2004. p. 1515–20. http://dx.doi.org/10.1109/ICIT.2004.1490789.

[12] Anand B, Jeyakumar A. Load frequency control of hydro-thermal system with fuzzy logic controller considering boiler dynamics. In: TENCON 2008 – 2008 IEEE region 10 conference; 2008. p. 1–5. http://dx.doi.org/10.1109/TENCON.2008.4766768.

[13] El-Metwally K. An adaptive fuzzy logic controller for a two area load frequency control problem. In: 12th International Middle-East Power System Conference, 2008. MEPCON 2008; 2008. p. 300–06. http://dx.doi.org/10.1109/MEPCON.2008.4562327.

[14] Shankar R, Chatterjee K, Chatterjee TK. Genetic algorithm based controller for load-frequency control of interconnected systems. In: 2012 1st international conference on Recent Advances in Information Technology (RAIT); 2012. p. 392–97. http://dx.doi.org/10.1109/RAIT.2012.6194452.

[15] Panda S, Yegireddy NK. Automatic generation control of multi-area power system using multi-objective non-dominated sorting genetic algorithm-ii. Int J Electr Power Energy Syst 2013;53:54–63. http://dx.doi.org/10.1016/j.ijepes.2013.04.003. http://dx.doi.org/10.1016/j.ijepes.2013.04.003.

[16] Bhatt P, Roy R, Ghoshal S. Ga/particle swarm intelligence based optimization of two specific varieties of controller devices applied to two-area multi-units automatic generation control. Int J Electr Power Energy Syst 2010;32(4):299–310. http://dx.doi.org/10.1016/j.ijepes.2009.09.004. <http://www.sciencedirect.com/science/article/pii/S014206150900146X>.

[17] Kumari N, Jha A. Particle swarm optimization and gradient descent methods for optimization of pi controller for agc of multi-area thermal-wind-hydro power plants. In: 2013 UKSim 15th international conference on computer modelling and simulation (UKSim); 2013. p. 536–541. http://dx.doi.org/10.1109/UKSim.2013.38.

[18] Ali E, Abd-Elazim S. Bacteria foraging optimization algorithm based load frequency controller for interconnected power system. Int J Electr Power Energy Syst 2011;33(3):633–8. http://dx.doi.org/10.1016/j.ijepes.2010.12.022. <http://www.sciencedirect.com/science/article/pii/S0142061511000044>.

[19] Abraham R, Das D, Patra A. Agc of a hydrothermal system with smes unit. In: GCC Conference (GCC), 2006 IEEE; 2006. p. 1–7. http://dx.doi.org/10.1109/IEEEGCC.2006.5686181.

[20] Parida M, Nanda J. Automatic generation control of a hydro-thermal system in deregulated environment. In: Proceedings of the eighth international conference on electrical machines and systems, 2005. ICEMS 2005, vol. 2, 2005. p. 942–47. http://dx.doi.org/10.1109/ICEMS.2005.202683.

[21] Khodabakhshian A, Hooshmand R. A new PID controller design for automatic generation control of hydro power systems. Int J Electr Power Energy Syst 2010;32(5):375–82. http://dx.doi.org/10.1016/j.ijepes.2009.11.006. http://dx.doi.org/10.1016/j.ijepes.2009.11.006.

[22] Moon Y, Ryu H, Lee J, Kim S. Power system load frequency control using noise-tolerable pid feedback. In: IEEE Int Symp Industrial Eletronics (ISIE), 2001; 2001. p. 1714–18.

[23] Zhang Y. Solving large-scale linear programs by interior-point methods under the matlab environment. Tech. rep., Department of Mathematics and Statistics, University of Maryland, Baltimore County, Baltimore, MD; July 1996.

[24] Mehrotra S. On the implementation of a primal-dual interior point method. SIAM J Optim 1992;2(4):575–601.

[25] Waltz RA, Morales JL, Nocedal J, Orban D. An interior algorithm for nonlinear optimization that combines line search and trust region steps. Math Program 2006;107(3):391–408. <http://link.springer.com/article/10.1007/s10107-004-0560-5>.

[26] IEEE Working Group on Prime Mover & Energy Supply Models for System Dynamic Performance Studies, Hydraulic turbine and turbine control models for system dynamic studies. IEEE Transactions on Power Systems No 17.